A DYNAMIC MODEL FOR THE TIME EVOLUTION OF THE MODULATED COSMIC RAY SPECTRUM

J. J. O'Gallagher and G. A. Maslyar III

May 1975

Technical Report # 75-079

(NASA-CR-142713) A DYNAMIC MODEL FOR THE TIME EVOLUTION OF THE MODULATED COSMIC RAY SPECTRUM (Maryland Univ.) 34 p HC $3.75 CSCL 04A

N75-23464

Unclas

G3/93 20998

UNIVERSITY OF MARYLAND

DEPARTMENT OF PHYSICS AND ASTRONOMY

COLLEGE PARK, MARYLAND

A DYNAMIC MODEL FOR THE TIME EVOLUTION OF THE MODULATED COSMIC RAY SPECTRUM

J. J. O'Gallagher and G. A. Maslyar III
Department of Physics and Astronomy
University of Maryland, College Park, Maryland 20742

May 1975

Technical Report # 75-079

ABSTRACT

A recently developed model predicts an energy dependent phase lag in the modulated cosmic ray density U(t) given by $U(t) \simeq U_s(t - \tau)$ where U_s is the solution to the Fokker-Planck equation under time independent conditions and τ is the average time spent by particles inside the modulating region. The delay times τ are functions of modulating parameters R (the radius of the modulating cavity), V (the solar wind velocity), and K (the effective average diffusion-coefficient which is a function of energy). This model is applied to predict the time evolution of the modulated cosmic ray proton spectrum over a simulated solar cycle. The predicted spectra reproduce most of the features of the so-called "hysteresis" effect when values of V = 360 km/sec, R = 60 a.u. and K varying between 1.3×10^{22} cm^2/sec at solar maximum and 3.5×10^{22} cm^2/sec at solar minimum are used. A modulation produced mostly by varying R over the solar cycle is less consistent with the observations.

A DYNAMIC MODEL FOR THE TIME EVOLUTION OF THE MODULATED COSMIC RAY SPECTRUM

J. J. O'Gallagher and G. A. Maslyar III
Department of Physics and Astronomy
University of Maryland, College Park, Maryland 20742

I. Introduction

The modulation of galactic cosmic ray nuclei with kinetic energies above a few tens of MeV/nucleon is qualitatively well understood in terms of the diffusion-convection picture originally proposed by Parker (1958, 1963), and later modified to include the effects of energy loss processes (Parker, 1965; Fisk and Axford, 1969; Fisk, 1971). In these models the spectrum for a particular epoch of the solar cycle is calculated by assigning specific values to a set of parameters assumed to characterize the state of the modulating region at that time. These parameters are chosen so that for an assumed interstellar spectrum the solution of the equilibrium or time-independent modulating equations fit the observed spectrum. The 11 year variation is then approximately reproduced by varying one or more of the modulating parameters and calculating the solutions under different stationary conditions. However when these "quasi-stationary" solutions are compared in some detail with observed variations at different energies, some features of the observed behavior cannot be reproduced without introducing several new parameters. For example, to explain the so-called "hysteresis" effect in which the relative modulation at different energies changes substantially between the phases of increasing and decreasing modulation as illustrated in Figure 1, it is necessary to introduce a diffusion coefficient which is an inseparable function of particle parameters and position and time coordinates. That is, the dependence of the diffusion coefficient on energy must be made to change with time or position or both and new parameters must be introduced.

As an alternative approach it has been shown recently (O'Gallagher 1973, 1975) that corrections for time variations in a dynamically evolving modulating region will lead naturally to a "hysteresis effect" without the need for additional parameters to characterize the "insep-arability" of the effective diffusion coefficient. Physically these corrections are a result of the fact that relatively large times may be required for some low energy particles to propagate from the inter-stellar medium by diffusion to the inner solar system. During this time the average medium characteristics are changing gradually. Thus particles with different propagation times will sample the average slowly changing modulating characteristics at different levels so that stationary solutions cannot be correct for all particles at the same time. It was shown first (O'Gallagher, 1973) that the corrections for this effect on the modulated density U(T,t) at kinetic energy T and time t can be simply expressed by

$$U(T,t) \cong U_s(T,t-\tau) \qquad (1)$$

where $U_s(T-\tau)$ is the equilibrium or stationary solution for energy T under conditions existing a time τ earlier.

By solving the full time dependent diffusion-convection equation, O'Gallagher (1975) (hereafter referred to as Paper I) showed that the delay time τ is in general a function of the usual modulating parameters, including the diffusion coefficient which is of course a function of energy. Thus this treatment predicts an energy dependent hysteresis effect without the need for exotic new modulating parameters.

It is the purpose of the paper to apply the concepts of this model to predict how the modulated spectra should evolve during an 11 year cycle and to show that these predictions reproduce quantitatively most observed features of the modulated spectra. In the process of this analysis, preliminary estimates for both the magnitude of the diffusion coefficient K_o (evaluated at a reference value of magnetic rigidity times velocity of $R\beta$ = 1GV) and the effective radius R of the modulating region are obtained.

II. Time-Lags and the "Hysteresis Effect"

Observations of the so-called hysteresis effect are conventionally presented in the form of regression plots of the intensity at some low energy versus the intensity at some higher reference energy such as illustrated in Figure 1. The effect can be concisely described by stating simply that in general the intensities at the two energies are related by a double-valued function. However there are two distinctly different physical interpretations of this fact:

1) Attributing the different relative levels of modulation to changes in the way the interplanetary medium depresses the intensity at different energies.

2) Attributing the failure of the low energy intensity to track the reference intensity to a real physical time-lag between the responses of the modulated intensities at different energies.

In the first interpretation above, the relevant observational parameter to characterize the hysteresis effect is the "hysteresis ratio", the ratio of the relative levels at low energy which are observed on the two branches of the regression curve at the same value of the reference intensity (Van Hollebeke, Wang and McDonald, 1972; Rygg, O'Gallagher and Earl, 1974). For example, in Figure 1 the regressions for the intensity at two different proton energies, ∿500 MeV and ∿100 MeV with respect to the Deep River neutron intensity show that this hysteresis ratio is energy dependent, varying from ∿1.9 at 100 MeV to ∿1.6 for ∿500 MeV protons. The effect was shown to be rigidity dependent by Van Hollebeke, et al (1973) who found values of 2.6 and 2.0 for the hysteresis ratio of 60 MeV/nucleon protons and helium respectively, and by Rygg, et al (1974) who found a somewhat smaller effect for the two species at higher energies.

In the second interpretation the explicit dependence of intensity on time is analyzed for both the low energy and the reference energy and the relevant parameter is the "time-lag" which must be introduced between the intensities at the two energies so that the loop in the regression between the intensities closes to approximate a single valued relationship.

The only quantitative analysis of hysteresis observations in terms of such time-lags was reported by Burger and Swanenburg (1973) for modulated electron intensities observed on OGO-5 with respect to the neutron intensity at Sulfur Mountain. These values are plotted in Figure 2 as a function of particle magnetic rigidity R times velocity β. Also plotted are the time-lags between the minimum neutron intensity at Deep River and the intensity minima for 60 MeV/nuc protons and helium estimated from the published data of Van Hollebeke, et al (1973). It should be noted that the phase lag τ is defined to have positive sign when the lower energy intensity lags that at higher energy (as is generally observed to be the case) and appears to be a smoothly decreasing function for $R\beta < 1$.

An analysis of time-lags between different neutron intensity monitors which resembled that discussed here was carried out by Simpson (1964), and Simpson and Wang (1967, 70). However in the latter works no evidence was found for significant lags between the neutron intensities at widely differing cut-off rigidities (this justifies the direct comparison of τ calculated with respect to different neutron monitors). Furthermore, the lags discussed there were between the modulated cosmic ray intensity in general and an index of solar activity (the coronal "green line") not between modulated intensities at different energies with respect to one another.

It should be emphasized that the physical basis for interpreting a "hysteresis ratio" and a "hysteresis phase lag" are fundamentally different. It is quite possible that both effects are present and that separation of the two may be quite difficult. However, despite the phenomenalogical description of hysteresis in terms of time-lags by some, virtually all of the attempts to explain the phenomena have been based solely on the first interpretation. For example, O'Gallagher (1969), Schmidt (1972), Van Hollebeke, et al (1972), Lezniak and Webber (1971), Burger and Swanenburg (1973), Bedijn, Burger and Swanenburg (1973), Van Hollebeke, et al (1973), and Rygg, et al (1974), all discuss in one way or another the description of the observations in terms of a change in the rigidity dependence of some "modulating function" in a time-independent model. On the other hand, the model developed in Paper I and discussed in the Introduction, provides for the first time a framework for the second interpretation by incorporating time-dependent diffusion and convection.

III. The Basic Three Parameter Model

The full time-dependent diffusion convection equation for the modulated cosmic ray density of a particular particle type is

$$\frac{K}{r^2}\frac{\partial}{\partial r}\left(r^2\frac{\partial U}{\partial r}\right) - \frac{V}{r^2}\frac{\partial}{\partial r}(r^2 U) + \frac{2V}{3r}\frac{\partial}{\partial T}(\alpha T U) = \frac{\partial U}{\partial t} \qquad (2)$$

where

$K = K(r,t,R,\beta)$ is the diffusion coefficient for a particle of velocity β and magnetic rigidity R at heliocentric radius r and time t

V is the solar wind velocity

and

$$\alpha = \frac{T + 2T_o}{T + T_o} \quad (T_o \text{ is the rest energy}).$$

In addition, we have made the following simplifying assumptions:

(1) The diffusion is isotropic (K is a scaler).

(2) The interplanetary medium is completely homogeneous (K and V are independent of heliocentric radius r), and

(3) The modulating cavity is spherically symmetric (with radius R).

In the conventional treatment the right hand side of equation (2) is set identically equal to zero and a form is assumed for the interstellar spectrum $U_o(T)$ and for the rigidity dependence of the diffusion coefficient $K = K_o\beta\, f(R)$ and a complete solution is numerically calculated on a computer. Such solutions are the "stationary solutions" U_s in equation (1) corresponding to particular values of R, V, and K_o (and, of course, $U_o(T)$ and $f(R)$).

In the treatment proposed in Paper I it was shown that from the solution of equation(2)including the time dependent term, one finds that the delay times τ appropriate for equation (1) are given by

$$\tau(R,V,K) = \left[\frac{R^2/K}{V^2/K + 36R^2} \right]^{1/2} \qquad (3)$$

Thus equations (1) and (3) provide a direct means of determining the parameters R, V and K in a way which does not involve assumptions about the form of the interstellar spectrum. For example, using a diffusion coefficient consistent with reported magnetic field power spectra (Jokipii and Coleman, 1968), and a solar wind velocity V = 360 km/sec, the delay times calculated as a function of $R\beta$ are plotted in Figure 3 for several different values of R. Note in particular that the predicted times have the limiting behavior that

$$\tau \approx R/V \qquad K \ll VR \qquad (4a)$$

and

$$\tau \approx R^2/6K \qquad K \gg VR \quad . \qquad (4b)$$

Also note that delays considerably longer than 6 months are possible under some conditions. The remarkable qualitative agreement between the predicted time delays (Figure 3) and those observed (Figure 2) provides considerable justification for continued analysis based on these concepts. Thus, based on this model, if one could measure τ accurately as a function of energy and time, and also monitor V at earth, one could determine

a) R as a function of time,

b) K(T,t) for K >> VR,

c) the absolute value of the "classical" modulating parameter $\eta = VR/K_o$ in the limit K >> VR as a function of time.

Note that the model does not introduce an additional time-variable parameter to characterize $f(R)$, but assumes that this form remains constant during the entire cycle. It was shown by Rygg, et al (1974) that if such a time variation is not introduced, other variations in R, V,and K_o will not produce a hysteresis in the stationary solutions. That is, the calculated spectra remain essentially unchanged for a wide range of R, V, and K_o, as long as the effective modulation characterized by the parameter $\eta = RV/K_o$ and the form of $f(R)$ are held constant.

It should also be noted that the solution derived in Paper I does not analytically include the effect on propagation times caused by the changes in K during propagation due to adiabatic energy loss processes. However it was shown here that such energy changes do not become important except in the low energy region where τ is independent of K. Thus adiabatic energy loss processes do not appreciably affect the delay times calculated from equation(3) on the basis of the energy (i.e. value of K) at which they are observed. The effects of these processes and other more complicated effects (e.g. radial propagation of non-uniformities in K due to convection) will lead to additional corrections which should be incorporated into more sophisticated time-dependent models.

To the extent that the idealized parameters R, V, and K can be related to real physical characteristics of the modulation, however this model provides a considerably more powerful means of determining them than other current models. It should be kept in mind that any real variation with time in effective dependence of the modulation on energy has been neglected in this approach. On the other hand, as long as diffusion is a good approximation to the mode of particle propagation the above effects must be present to some degree.

Unfortunately, accurate measures of τ over a wide range of particle parameters and long time intervals do not yet exist so that applications of the model must be relatively crude at present.

In the present work, we will use observed data to choose reasonable values for each of the three parameters and calculate the stationary proton spectra at various times during a simulated solar cycle. We then use equation (3) to determine the time-lags as a function of energy and time, and correct these spectra by a simple linear interpolation between stationary spectra calculated at two different times. We will then compare the corrected spectra with hysteresis observations. All of the stationary spectra derived below are computed from a program developed by Fisk (1971) applied to an assumed interstellar spectrum which is a power law in total energy ($U_o(T) \propto (T+T_o)^{-2.6}$) and calculated for $f(R) = R$ in GV so that $K = K_o \times R\beta$ (K_o in cm^2/sec for $R\beta$ in GV).

IV. Calculation of Spectra

Choice of Parameter Values. We wish first to select values for V,R, and K_o which are consistent with current observations and conventional analyses.

The choice for V is relatively straight-forward since observations over a large portion of a solar cycle have not revealed any systematic variations in the average solar wind velocity sufficient to account for observed modulation (Gosling, Hansen and Bame, 1971). Therefore we shall assume this parameter remains constant in time and chose a value of V = 360 km/sec which is the value found by Smith (1974), to give the Archimedes spiral which most closely approximates the average magnetic field behavior observed on Pioneer 10.

To determine R near solar maximum consistent with the model we invoke equation (4a) and compare it with observed time-lags at small diffusion coefficient (small $R\beta$) from Figure 2. All of the observed lags for $R\beta \leq 1$ GV are consistent with $\tau \cong 280 \pm 70$ days $\cong R/V$. With the above value for V this yeilds $R \cong 60$ a.u.

With these values of V and R, the value of the diffusion coefficient which best fits the 1969 (Solar Maximum) proton spectrum is determined to be $K_o = 1.3 \times 10^{22}$ cm^2/sec. The observed and calculated spectra are shown in Figure 4. Since we have deliberately kept the model simple the fit is not ideal at all energies. In particular, the observed direct proportionality between intensity J and energy T (J = AT) reported by Rygg and Earl (1973) is not accurately reproduced consistent with the intensity at higher energies. However, this discrepancy is a well known feature of computed spectra based on such simple parameter models and has been discussed extensively (Fisk, Forman and Axford, 1973). For the purposes of this study it is not important since we are mainly interested only in the overall level of modulation and how the relative levels vary with time. The values of the three parameters correspond to $\eta = 2.5$ at solar maximum and a similar fit gives $\eta = 0.9$ at solar minimum in 1965 with $K_o = 3.6 \times 10^{22}$ cm^2/sec as also shown in Figure 4.

Stationary Spectra. The variation in η between solar maximum and minimum can be the result of a variation in either R or K or both. For simplicity we have considered the effect of variations of each separately. The two spectra in Figure 4 and the corresponding values of the modulating parameters have been taken to be the extremes of a nominal 10 year solar cycle. Assuming that the cycle is symmetric and that the parameter η varies linearly with time between these extremes we have generated 4 intermediate stationary spectra first by varying K_o and then by varying R. The spectra are virtually identical in the two cases since the form of f(R) was not changed. Thus there is no way of distinguishing between an R or K_o variation on the basis of the stationary spectra. The full complement of spectra for the case of K_o varying but R and V constant is shown in Figure 5, and selected points calculated for varying R with K_o constant are indicated by X's. For a 10 year cycle beginning at solar minimum in year 0, the individual stationary spectra for each year are numbered from 0-9 in the Figure. Note that there is no "hysteresis" since the stationary spectra at a particular level of modulation at high energies (e.g. years 2 and 8) are identical at all energies.

Corrected Spectra. The time delays expected from diffusive propagation can be calculated directly from equation (3) as a function of energy for each spectrum in Figure 5. Families of curves illustrating these times for the cases of K_o variation and R variation are shown in Figure 6 (a and b). Note that there is considerable difference in the time variation of τ in the two cases which in principle would allow us to distinguish between R or K_o variation.

Since the intensity J is related to the density U by $J = \frac{\beta c U}{4\pi}$ we can simply rewrite equation (1) for J as

$$J(T,t) \cong J_s(T,t-\tau)$$
$$\cong J_s(T,t) - \frac{\Delta J_s}{\Delta t}\tau \quad . \tag{5}$$

It is then a simple procedure to interpolate between to stationary spectra assumed separated by a year (Δt = 365 days) to determine the corrected intensity J(T,t) by inserting the appropriate value of τ from Figure 6 in equation (5).

The full range of spectra which have been synthesized by this procedure for the case of K_o varying, R = constant (Figure 6a) are shown in Figure 7.

Many aspects of observed hysteresis phenomenon are immediately evident in Figure 7. Note in particular the following

(1) The intensity at lower energies always lags that at

higher energies (as observed) as a general consequence of the model. Models which explain hysteresis by varying f(R) do not predict the direction of the effect.

(2) The corresponding spectra in opposite phases of the modulation (e.g. years 4 and 7) actually cross as observed (Rygg, et al, 1974). Models which vary f(R) produce this effect near solar maximum by increasing the modulation at low energies at the same time as it is decreasing at high energies.

(3) At the same level of modulation at high energies (e.g. spectra for years 1 and 9) the spectra diverge gradually as one goes to low energies which is the observed qualitative feature discussed in detail by Rygg, et al (1974).

While each of these features can be reproduced by models which vary f(R), they emerge naturally from the present model. Variations in f(R) require a particular systematic variation of the interplanetary power spectrum (a spectral exponent which steepens as one passes through a solar maximum) which, although it may occur, has not been observed. In addition, it requires new parameters to describe and new physics to explain.

V. Hysteresis "Loops"

In Figure 8 a, b, and c, calculated regressions for the intensity at three low energy intervals with respect to that at 10 BeV are shown and compared with the observations. In each case the spectra in Figure 5 yield a single-valued regression. The low energy intensities are corrected for the propagation delays τ from

Figure 6a (R = const, K varying) using equation (5).

Consider first the predicted behavior for 100 MeV protons in Figure 8a. Two regression loops are shown. The dashed curve is based on a symmetric 10 year cycle. That is Δt in equation (5) is assumed to be 1 year between each of the 6 spectra in Figure 5 which give the single valued regression shown. The resulting loop agrees well with the observations from solar minimum to solar maximum (upper branch) but lies closer to the single valued regression than the observations on the lower branch. As a more accurate application of the model we note, however, that the actual solar cycle which we are analyzing was not symmetric nor did it last 10 years. After cosmic ray maximum in May 1965, the general level decreased gradually until 1969-70, which is considered to be the most recent solar maximum. Then intensities recovered rather rapidly, so that by late 1972 most indices were back to nearly the 1965 levels. Accordingly we have also calculated expected regressions for a more accurate approximation to the true cycle described by a 4 year declining phase from solar minimim to maximum (1965-1969) and a 3 year recovery (1969-1972). Thus Δt in equation (5) was 292 days and 219 days respectively during the depression and recovery phases. The resulting loop fits the data extremely well. Note in particular that the calculated regression has a pronounced segment of negative slope near solar maximum. The importance of this observed feature was discussed by Rygg, et al (1974). The agreement is quantitative as well as qualitative in that the two branches are related by a factor of $\sim$1.9 as observed (see Figure 1).

The difference between the two calculated loops and the better argreement attained by the latter serves to emphasize that the correction given by equation(5)depends not only on the phase lag τ, but also on the rate dJ/dt at which the spectrum is changing. In particular, note that one prediction of the model is that if a period of relatively constant intensity is maintained for longer than τ, hysteresis loops should close. The regressions calculated in Figure 8b and c have all been derived for the more representative approximation to the actual cycle.

In Figure 8b we show the data of Van Hollebeke, et al (1972) and the calculated regression produced by varying K with R constant (dashed curve). Again the agreement is excellent showing the proper spread between upper and lower branches as well as the segment of negative slope. Also shown in Figure 8b is the regression calculated for phase lags which would be expected if K_o were held constant and R varied (Figure 6b). It would appear that the short delays predicted in a small region at solar minimum are not consistent with the observations.

Finally in Figure 8c are shown the calculated and observed regressions for 500 MeV protons. Here, although relatively good agreement is attained during the declining phase and near maximum, during the recovery phase the effect is about 60% larger than predicted. This discrepancy is perhaps due to the simplicity of the three parameter model and the possibility that some assumptions are inaccurate. For instance, the value of K used here was based on a) an assumed diffusion coefficient $K = K_o R\beta$, and b) as assumed interstellar spectrum which is a power law in total energy. An inaccuracy in either or both of these assumptions could easily account for a diffusion coefficient about 60% smaller than used here which would remove the discrepancy without affecting the lower energy results. It would however imply a correspondingly larger value of η which in turn would suggest that U_o at $\sim$500 MeV was somewhat higher than the power law in total energy assumed. Neither the observations nor the simplified modulation model used here can allow such a conclusion to be drawn unambiguously at the present time.

VI. Summary and Conclusions

The analysis and comparison with observations in the foregoing sections has demonstrated that a model incorporating the effects of diffusive propagation delays, provides a completely self-consistent explanation of the so called "hysteresis effect". In particular, the following features are specifically predicted as observed.

(1) The "cross over" of modulated spectra observed in two successive years on either side of solar maximum.

(2) The splitting towards lower energies of the spectra modulated at the same level at high energies.

(3) The segment of negative slope observed in some regression near solar maximum.

(4) The direction of the effect (the fact that lower energies lag higher energies in time).

In addition to this qualitative agreement, the model provides excellent quantitative agreement with the observations when applied for the actual time behavior in the solar cycle. This agreement is achieved without introducing <u>any</u> new free parameters. Imposing self-consistency with estimates of the overall level of the modulation provides in fact a crude determination of these parameters. Starting with only the assumptions of a constant solar wind velocity V = 360 km/sec and an interstellar spectrum which is a power law in total energy, application of the model leads to the following tentative conclusions:

1) The effective size of the modulating cavity at solar maximum in 1969-70 was $R \cong 60$ a.u. (within about $\pm$ 25%).

2) The effective diffusion coefficent for particles with $R\beta = 1$ GV at solar maximum was $K_o = 1.3 \times 10^{22}$ cm^2/sec (also with an accuracy of about $\pm$ 25%).

3) The value of the modulating parameter η varied from 2.5 at solar maximum to 0.9 at solar minimum.

4) Much of the variation in η was due to variation in effective diffusion coefficient K rather than size of the modulating cavity.

It is worth noting that the parameters above would predict a gradient for 1 BeV protons of $\frac{1}{U}\frac{\partial U}{\partial r} = \frac{V}{K(1\ \text{BeV})} = 3\%$/a.u. which is in excellent agreement with the integral gradients observed on Pioneer 10 (see McKibben, 1975)for particles with a median energy of $\sim$ 1 BeV/nucleon. On the other hand, the observation of a hysteresis effect for 500 MeV protons which is about 60% larger than predicted by the above assumptions would indicate that the above estimate of K_o may be high and the estimate of η (and therefore the corresponding gradient and true interstellar spectrum) low by perhaps a factor of $\gtrsim$ 2.

Continued monitoring of the modulated intensity over a wide range of energies during the entire cycle will provide the data from which a conclusive test of the validity of these concepts can be made. Should they continue to be as succesful at explaining the more precise observations as for current observations, then they have potential to provide, in addition, a continuous monitor of the modulation parameters themselves and a definitive reconstruction of the interstellar proton spectrum above ∿500 MeV.

Acknowledgements: We are indebted to Dr. Leonard Fisk for providing the computer programs used in this analysis. Also we wish to thank the Computer Science Center of the University of Maryland for supporting this work in part through the provision of computer time. In addition this work was supported by NASA Grant NGR 21-002-316.

References

Bedijn, P. J., J. J. Burger, and B. N. Swanenburg, The long term modulation of cosmic rays, Proc. Int. Conf. Cosmic Rays 13th, 5, 3106, 1973.

Burger, J. J., and B. N. Swanenburg, Energy dependent time-lag in the long term modulation of cosmic rays, J. Geophys. Res., 78, 292, 1973.

Fisk, L. A., Solar modulation of galactic cosmic rays, 2, J. Geophys. Res., 76, 221, 1971.

Fisk, L. A., and W. I. Axford, Solar modulation of galactic cosmic rays, 1, J. Geophys. Res., 74, 4973, 1969.

Fisk, L. A., M. A. Forman, and W. I. Axford, Solar modulation of galactic cosmic rays, 3, Implications of the Compton-Getting coefficient, J. Geophys. Res., 78, 995, 1973.

Gosling, J. T., R. T. Hansen, and S. J. Bame, Solar wind speed distributions: 1962-1970, J. Geophys. Res., 76, 1811, 1971.

Jokipii, J. R., and P. J. Coleman, Cosmic ray diffusion tensor and its variation observed with Mariner 4, J. Geophys. Res., 73, 5495, 1968.

Lezniak, J. A., and W. R. Webber, Solar modulation of cosmic ray protons, helium nuclei and electrons: a comparison of experiment with theorys, J. Geophys. Res., 76, 1605, 1971.

McKibben, R. B., Cosmic ray intensity gradients in the solar system, (to be published in Reviews of Geophys. and Space Phys.) 1975.

O'Gallagher, J. J., Analysis of changes in the modulated cosmic ray spectrum near solar minimum, J. Geophys. Res., 74, 43, 1969.

O'Gallagher, J. J., Cosmic ray hysteresis as evidence for time-dependent diffusive processes in the long term solar modulation, Proc. Int. Conf. Cosmic Rays 13th, 2, 1135, 1973.

O'Gallagher, J. J., A time-dependent diffusion-convection model for the long term modulation of cosmic rays, Astrophys. J., , , 1975.

Parker, E. N., Cosmic ray modulation by solar wind, Phys. Rev., 110, 1445, 1958.

Parker, E. N., Interplanetary Dynamical Processes, pp. 196-206, John Wiley, New York, 1963.

Parker, E. N., The passage of energetic charged particle through interplanetary space, Planet. Space Sci., 13, 9, 1965.

Rygg, T. A. and J. A. Earl, Balloon measurements of cosmic ray protons and helium over half a solar cycle, 1965-1969, J. Geophys. Res., 76, 7445, 1971.

Rygg, T. A., J. J. O'Gallagher and James A. Earl, Modulation of cosmic ray protons and helium nuclei near solar maximum, J. Geophys. Res., 79, 4129, 1974.

Schmidt, P. J., Cosmic ray electron spectrum and its modulation near solar maximum, J. Geophys. Res., 77, 3295, 1972.

Simpson, J. A., Primary cosmic ray spectrum and the transition region between interplanetary and interstellar space, Proc. Int. Conf. Cosmic Rays 8th, 2, 155, 1964.

Simpson, J. A. and J. R. Wang, Dimension of the cosmic ray modulation region, Astrophys. J. (Letters), 149, L73, 1967.

Simpson, J. A. and J. R. Wang, The eleven-year and residual solar modulation of cosmic rays (1952-1969), Astrophys. J., 161, 265, 1970.

Smith, E. J., Radial gradients in the interplanetary magnetic field between 1.0 and 4.3 AU: Pioneer 10, Solar Wind Three, Ed. C. T. Russel, IGPP, UCLA, 257, 1974.

Van Hollebeke, M. A. I., J. R. Wang and F. B. McDonald, The modulation of low-energy galactic cosmic rays over solar maximum (cycle 20), J. Geophys. Res., 77, 6881, 1972.

Van Hollebeke, M. A. I., J. R. Wang, and F. B. McDonald, The modulation of low energy galactic cosmic rays, Proc. Int. Conf. Cosmic Ray 13th, 2, 1298, 1973.

FIGURE CAPTIONS

FIGURE 1. Observed regressions for Cosmic Ray Protons versus Neutron Intensity exhibit the double-valued "hysteresis effect". The data are from a series of balloon flights covering most of a complete solar cycle (Rygg and Earl, 1971, Rygg et al 1974).

FIGURE 2. The modulated intensity of low rigidity particles appears to "lag" the intensity at higher rigidity (as measured by neutron monitors) by delay times of up to more than 30 days. The electron and integral proton measurements (Burger and Swanenburg, 1973) clearly show a gradually shortening of the delay with increasing rigidity. The low rigidity proton and helium points are from the data of Van Hollebeke, et al (1972).

FIGURE 3. Predicted delay times calculated from equation 3. For illustration we have used a diffusion coefficient consistent with interplanetary magnetic field power spectra. The curves shown are qualitatively similar to the observed times shown in Figure 2.

FIGURE 4. Data for protons observed near solar maximum and solar minimum are shown together with computed spectra based on the modulation parameters indicated. The individual measurements were compiled from a number of sources by Rygg, et al (1974). The calculated spectra were based on an assumed unmodulated spectrum having the form of a power law in total energy.

FIGURE 5. Calculated stationary or time-independent spectra for each year of a symmetric 10 year solar cycle. The spectra were calculated by assuming the modulating parameter $\eta = VR/K_o$ varies linearly with time between the solar maximum and minimum spectra in Figure 4 and the curves shown are for V and R constant with K_o varying. Selected points for V and K constant while R varies are shown by the X's. The diffusion coefficient was assumed to be proportional to $R\beta$ for all spectra so no "hysteresis" is generated.

FIGURE 6. Delay times calculated to correct the spectra in Figure 5 based directly on the values of R, V, and K used to generate those spectra. a) constant R, variable K_o, b) constant K_o, variable R.

FIGURE 7. Calculated Spectra corrected for propagation delays. The spectra exhibit all observed features of the "hysteresis effect" as discussed in the text.

FIGURE 8a. The corrected intensities exhibit hysteresis loops which are similar to the observed loops. The best fit is attained when a cycle made up of a 4 year decling phase and a 3 year recovery (heavy dotted lines) is used rather than a symmetric 10 year cycle (5 year declining and recovery phases shown by the light dashed curve).

FIGURE 8b. The loop calculated from the model for 60 MeV protons relative to high energies agrees well with the observations if the times are based on a constant radius with K_o variable.

FIGURE 8c. The predicted times from Figure 6a are not long enough to produce all of the observed hysteresis at 500 MeV but this simply indicates that the actual diffusion coefficient may be slightly smaller than used here in our simple model at these energies.

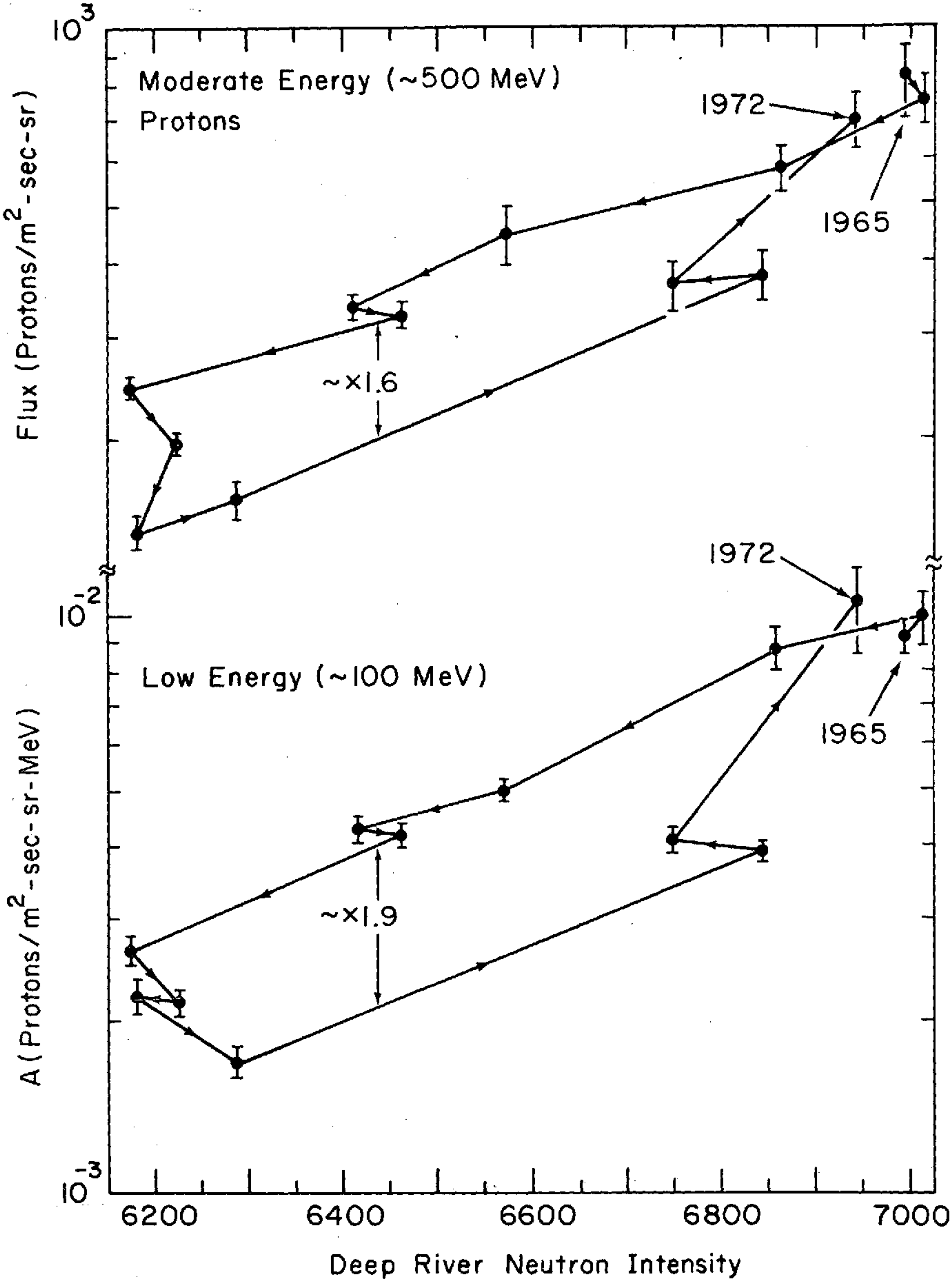

Moderate Energy (~500 MeV)
Protons
1972
1965
~×1.6
Low Energy (~100 MeV)
1972
1965
~×1.9
Flux (Protons/m²-sec-sr)
A (Protons/m²-sec-sr-MeV)
10³
10⁻²
10⁻³
6200
6400
6600
6800
7000
Deep River Neutron Intensity

FIGURE 1

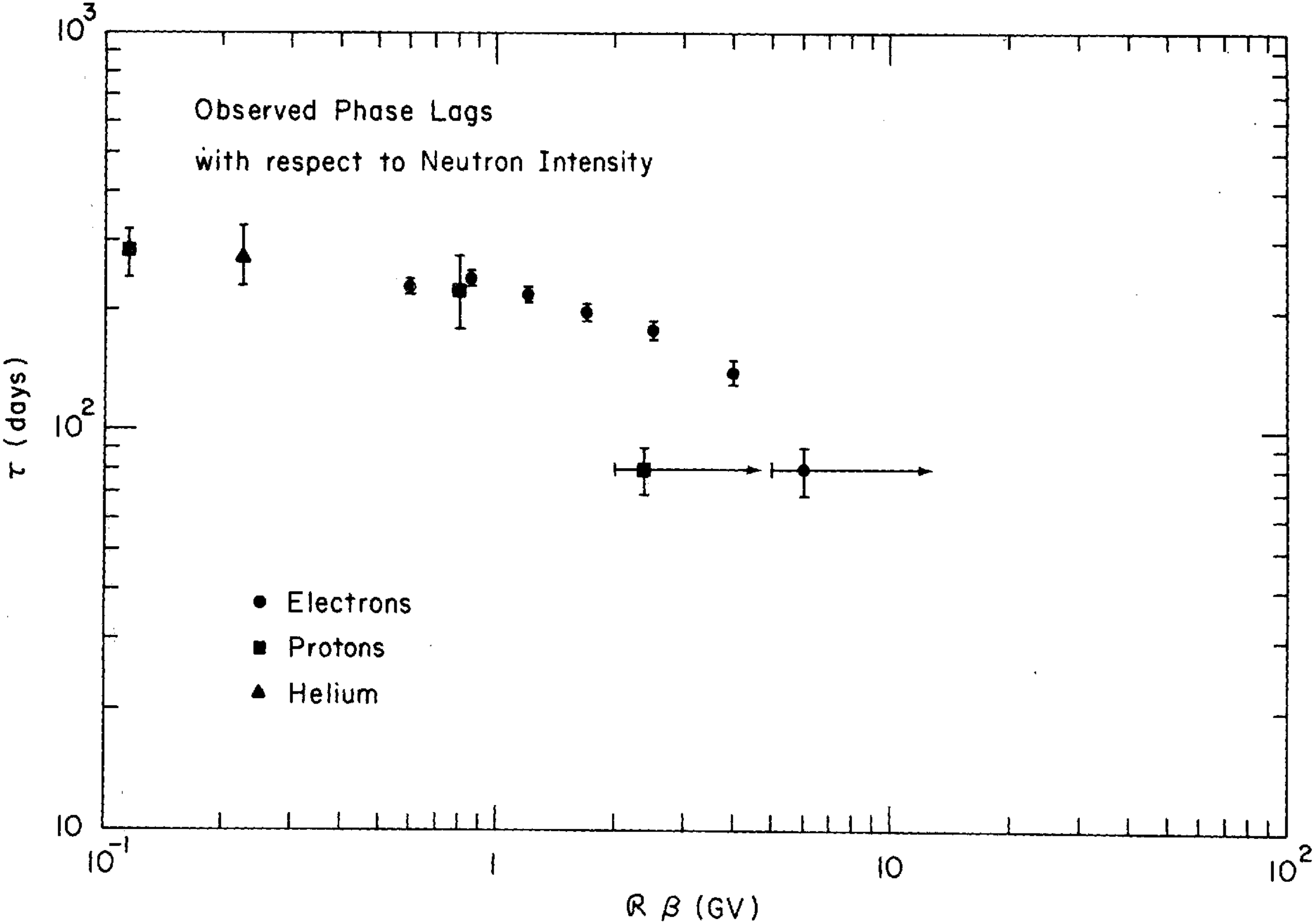

Observed Phase Lags
with respect to Neutron Intensity
Electrons
Protons
Helium
τ (days)
R β (GV)
10
10^2
10^3
10^-1
1
10
10^2

FIGURE 2

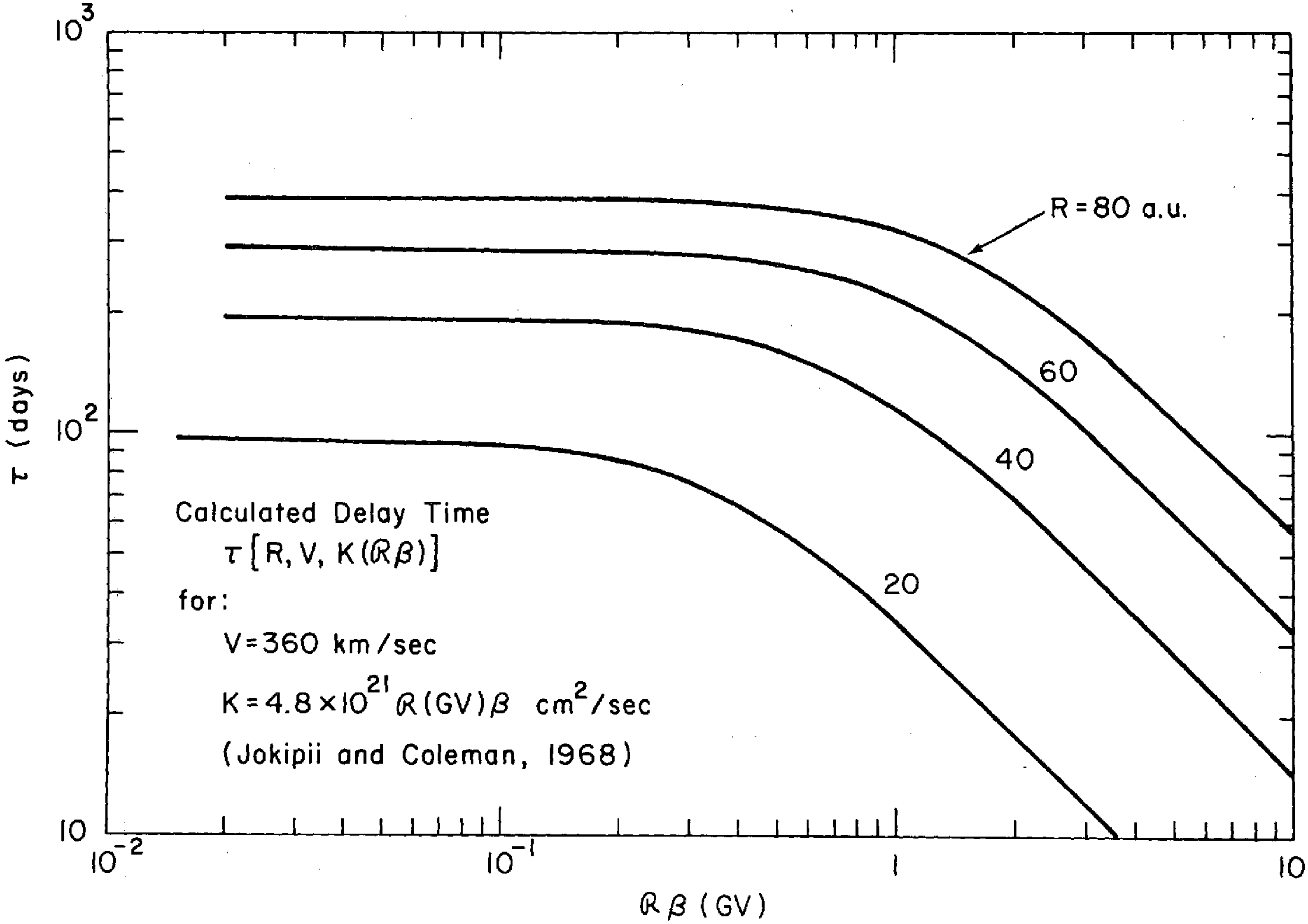

10^3
10^2
10
τ (days)
R = 80 a.u.
60
40
20
Calculated Delay Time
$\tau[R, V, K(\mathcal{R}\beta)]$
for:
V=360 km/sec
$K = 4.8 \times 10^{21} \mathcal{R}(GV)\beta \; cm^2/sec$
(Jokipii and Coleman, 1968)
10^{-2}
10^{-1}
1
10
$\mathcal{R}\beta$ (GV)

FIGURE 3

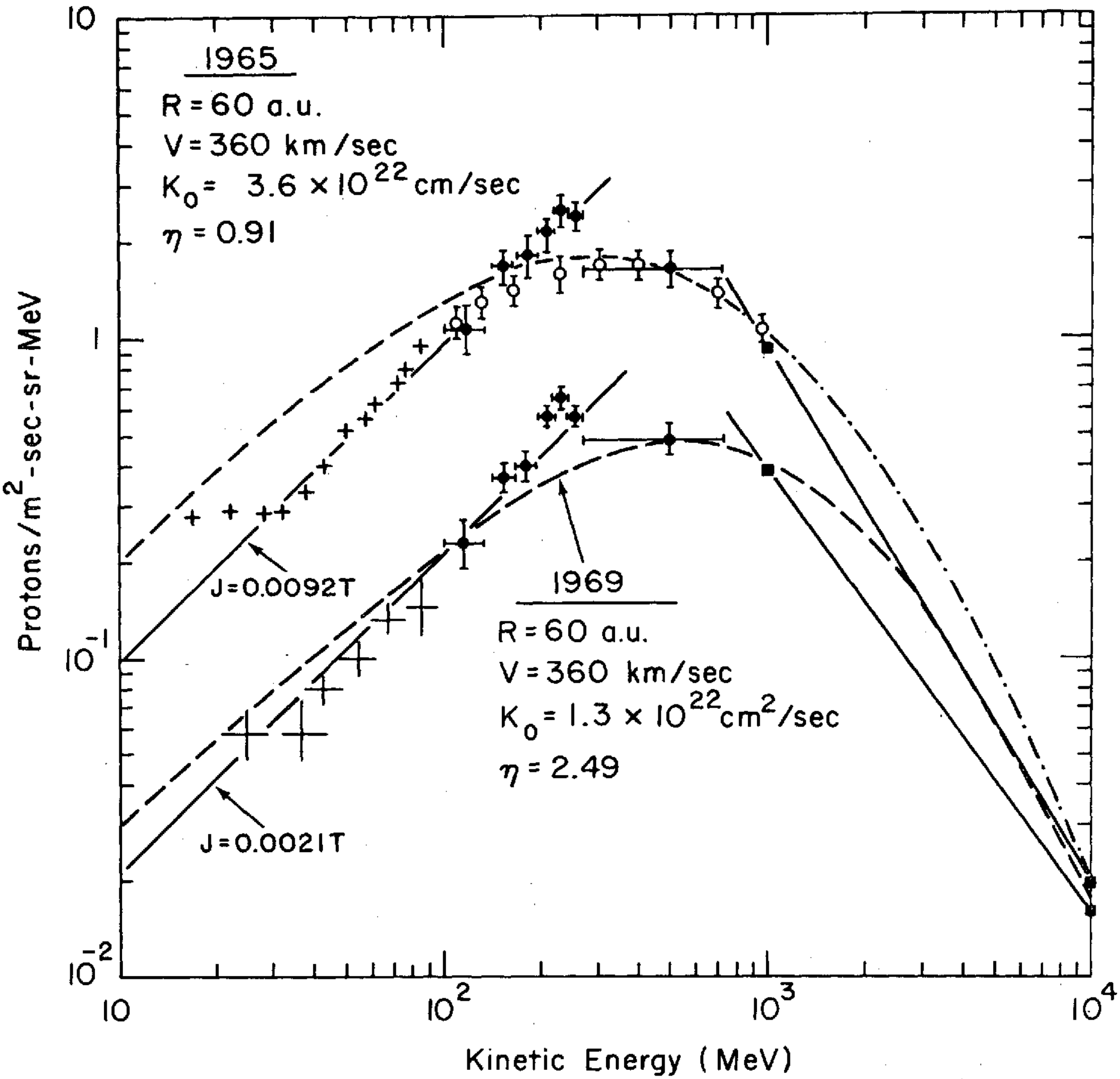

1965
R = 60 a.u.
V = 360 km/sec
K0 = 3.6 × 10^22 cm/sec
η = 0.91
J=0.0092T
1969
R = 60 a.u.
V = 360 km/sec
K0 = 1.3 × 10^22 cm^2/sec
η = 2.49
J=0.0021T
Protons/m^2-sec-sr-MeV
Kinetic Energy (MeV)
10
1
10^-1
10^-2
10
10^2
10^3
10^4

FIGURE 4

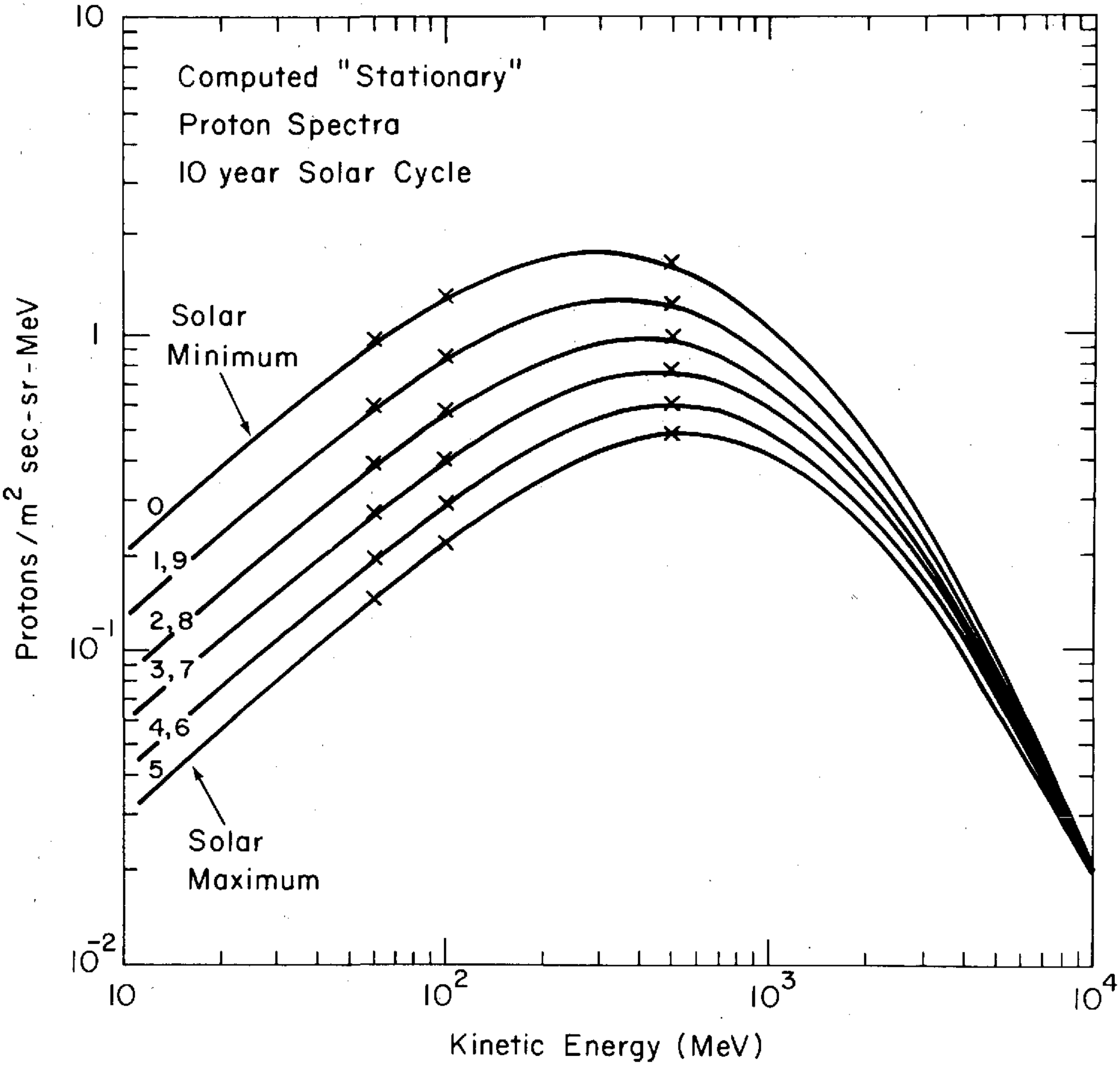

Computed "Stationary"
Proton Spectra
10 year Solar Cycle
Solar
Minimum
0
1,9
2,8
3,7
4,6
5
Solar
Maximum
Protons / m² sec-sr-MeV
Kinetic Energy (MeV)
10
1
10^{-1}
10^{-2}
10^2
10^3
10^4

FIGURE 5

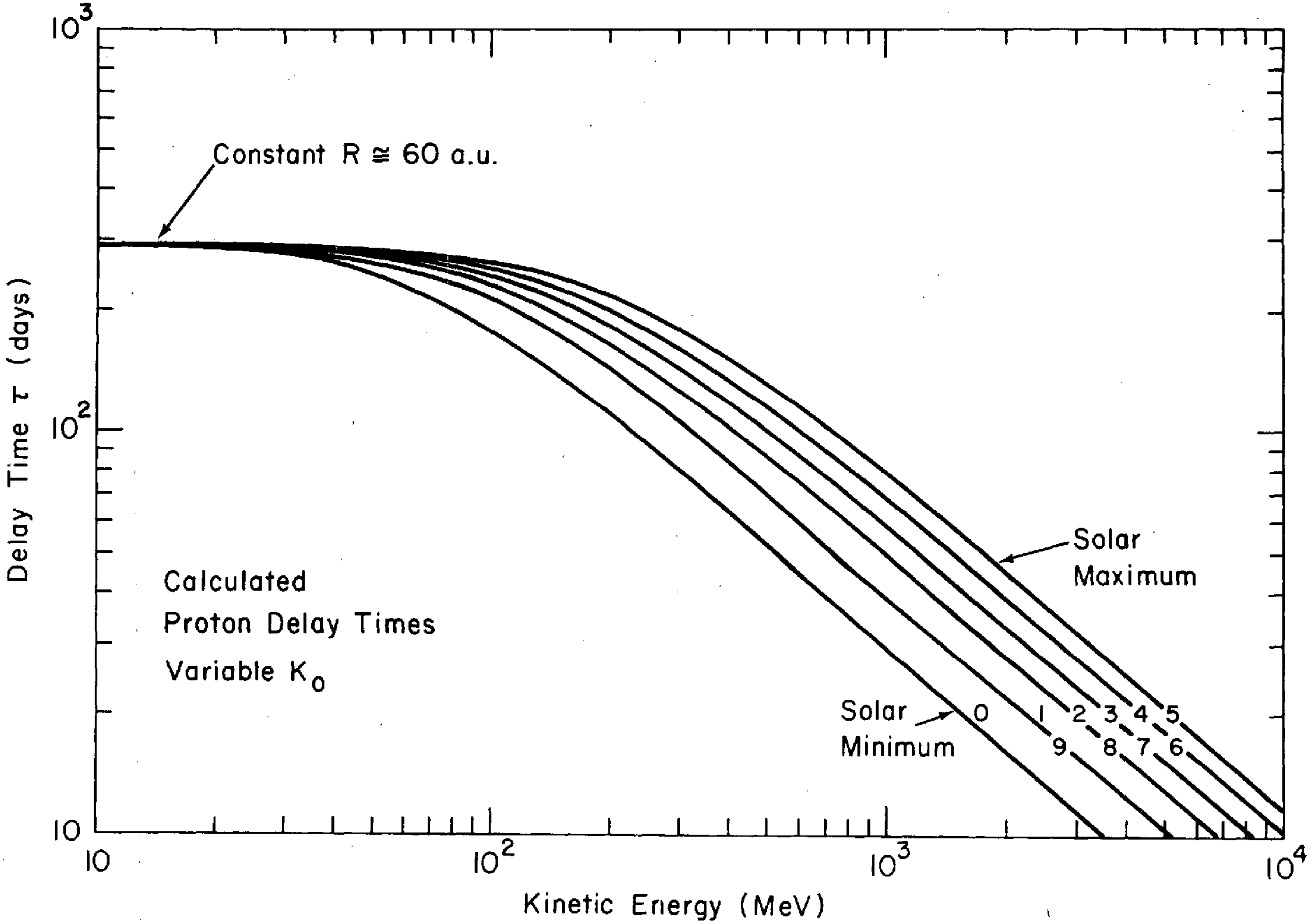

Constant R ≅ 60 a.u.
Delay Time τ (days)
Calculated
Proton Delay Times
Variable K_o
Solar Maximum
Solar Minimum
0 1 2 3 4 5
9 8 7 6
10^3
10^2
10
10
10^2
10^3
10^4
Kinetic Energy (MeV)

FIGURE 6a

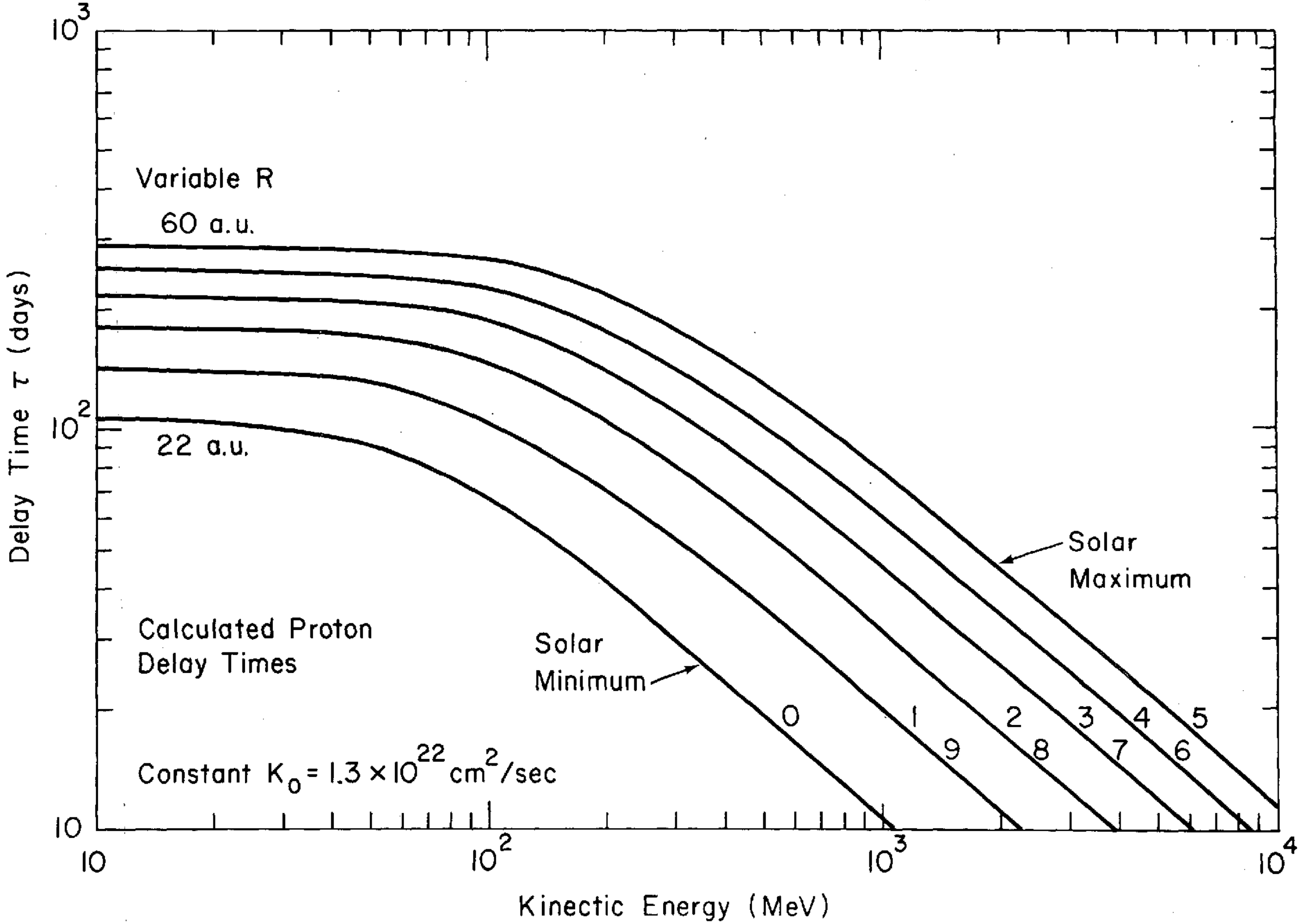
Variable R
60 a.u.
22 a.u.
Calculated Proton
Delay Times
Constant $K_0 = 1.3 \times 10^{22}$ cm^2/sec
Solar Maximum
Solar Minimum
0
1
9
2
8
3
7
4
6
5
Delay Time τ (days)
Kinectic Energy (MeV)
10^3
10^2
10
10
10^2
10^3
10^4

FIGURE 6b

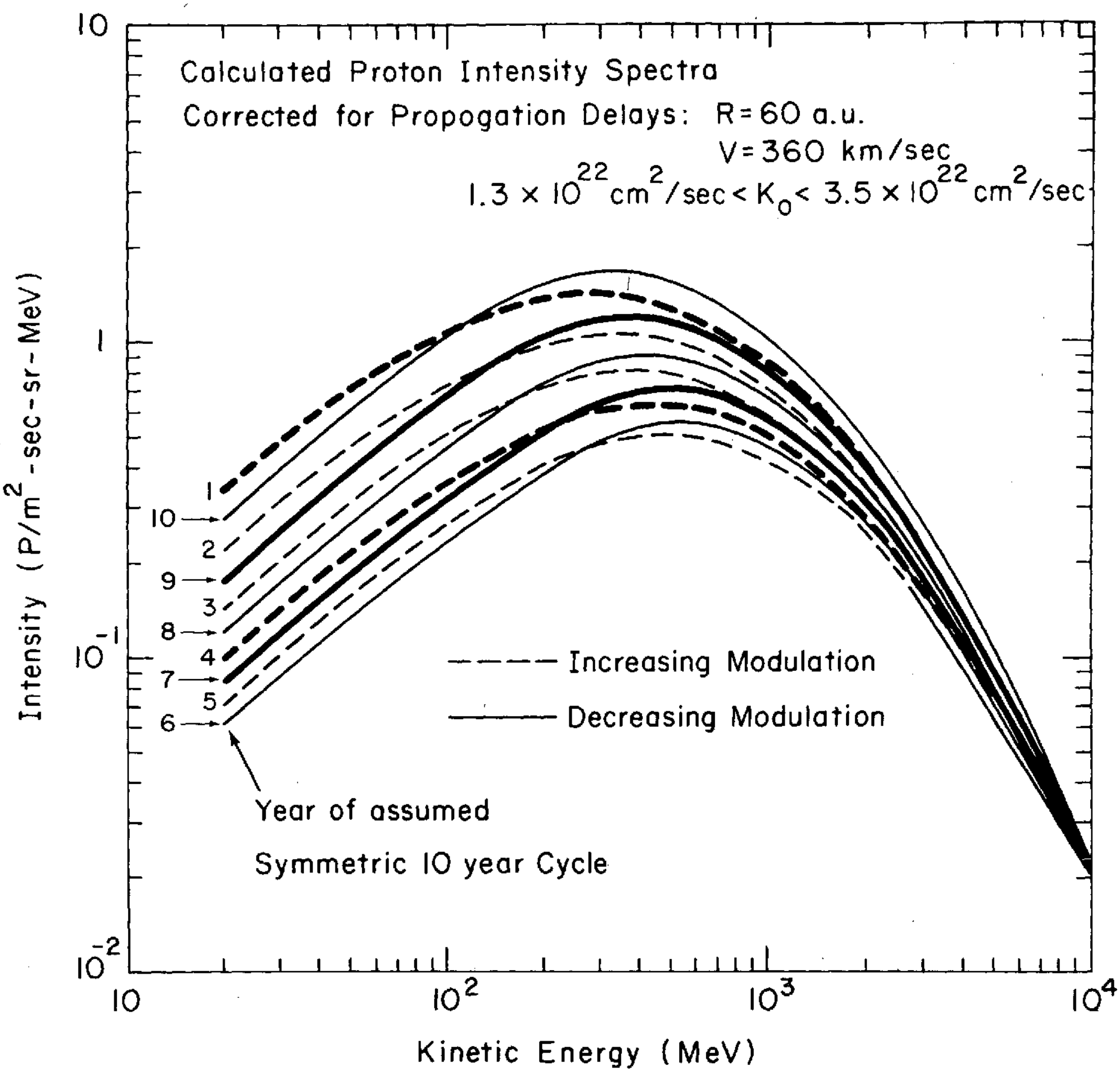
Calculated Proton Intensity Spectra
Corrected for Propogation Delays: R = 60 a.u.
V = 360 km/sec
1.3 × 10^22 cm^2/sec < K_0 < 3.5 × 10^22 cm^2/sec
Intensity (P/m^2-sec-sr-MeV)
Kinetic Energy (MeV)
10
1
10^-1
10^-2
10
10^2
10^3
10^4
1
10
2
9
3
8
4
7
5
6
Increasing Modulation
Decreasing Modulation
Year of assumed
Symmetric 10 year Cycle

FIGURE 7

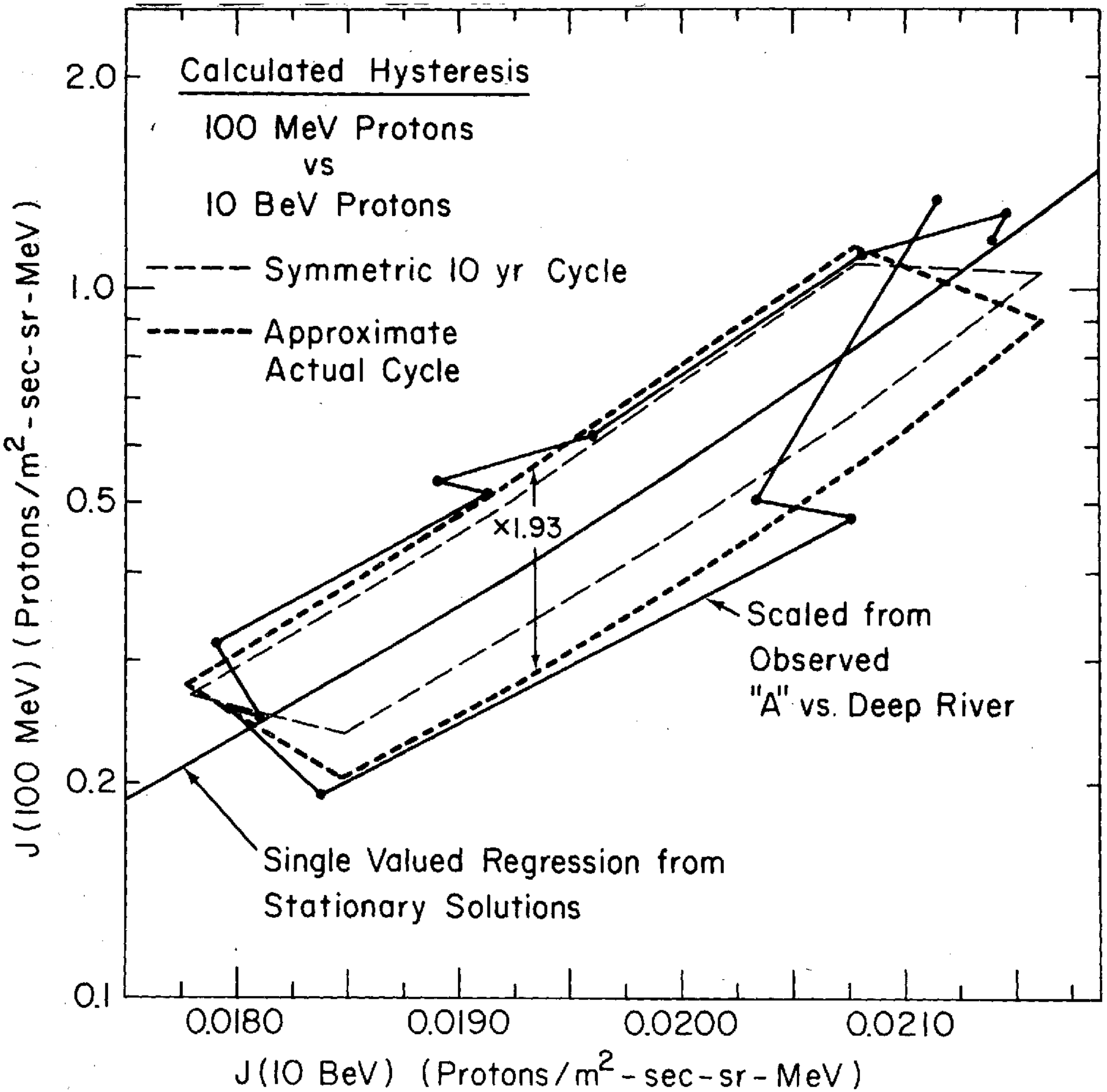

Calculated Hysteresis
100 MeV Protons
vs
10 BeV Protons
Symmetric 10 yr Cycle
Approximate
Actual Cycle
×1.93
Scaled from
Observed
"A" vs. Deep River
Single Valued Regression from
Stationary Solutions
2.0
1.0
0.5
0.2
0.1
0.0180
0.0190
0.0200
0.0210
J (100 MeV) (Protons/m2-sec-sr-MeV)
J (10 BeV) (Protons/m2-sec-sr-MeV)

FIGURE 8a

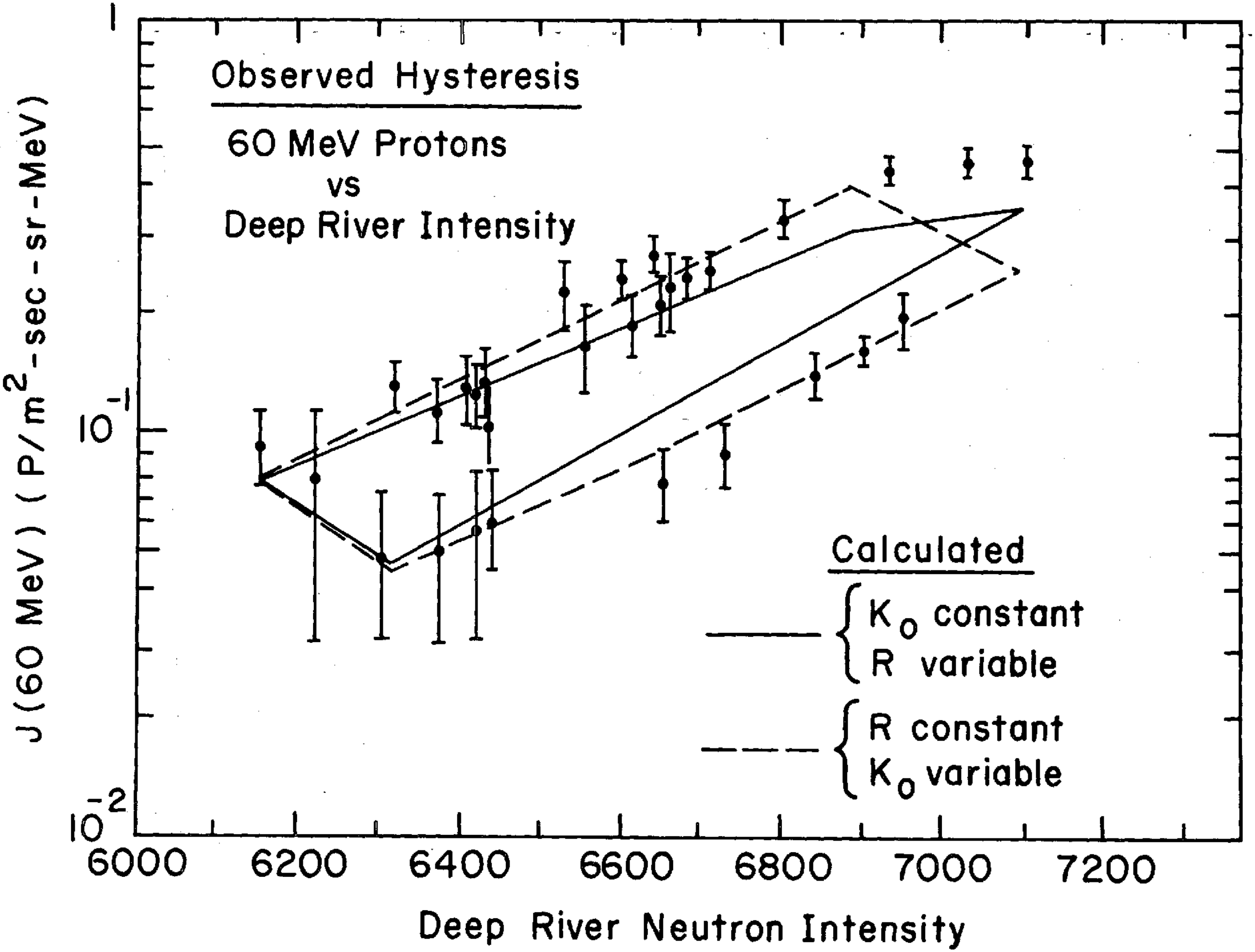
Observed Hysteresis
60 MeV Protons
vs
Deep River Intensity
Calculated
K$_0$ constant
R variable
R constant
K$_0$ variable
J (60 MeV) (P/m^2-sec - sr - MeV)
1
10^{-1}
10^{-2}
6000
6200
6400
6600
6800
7000
7200
Deep River Neutron Intensity

FIGURE 8b

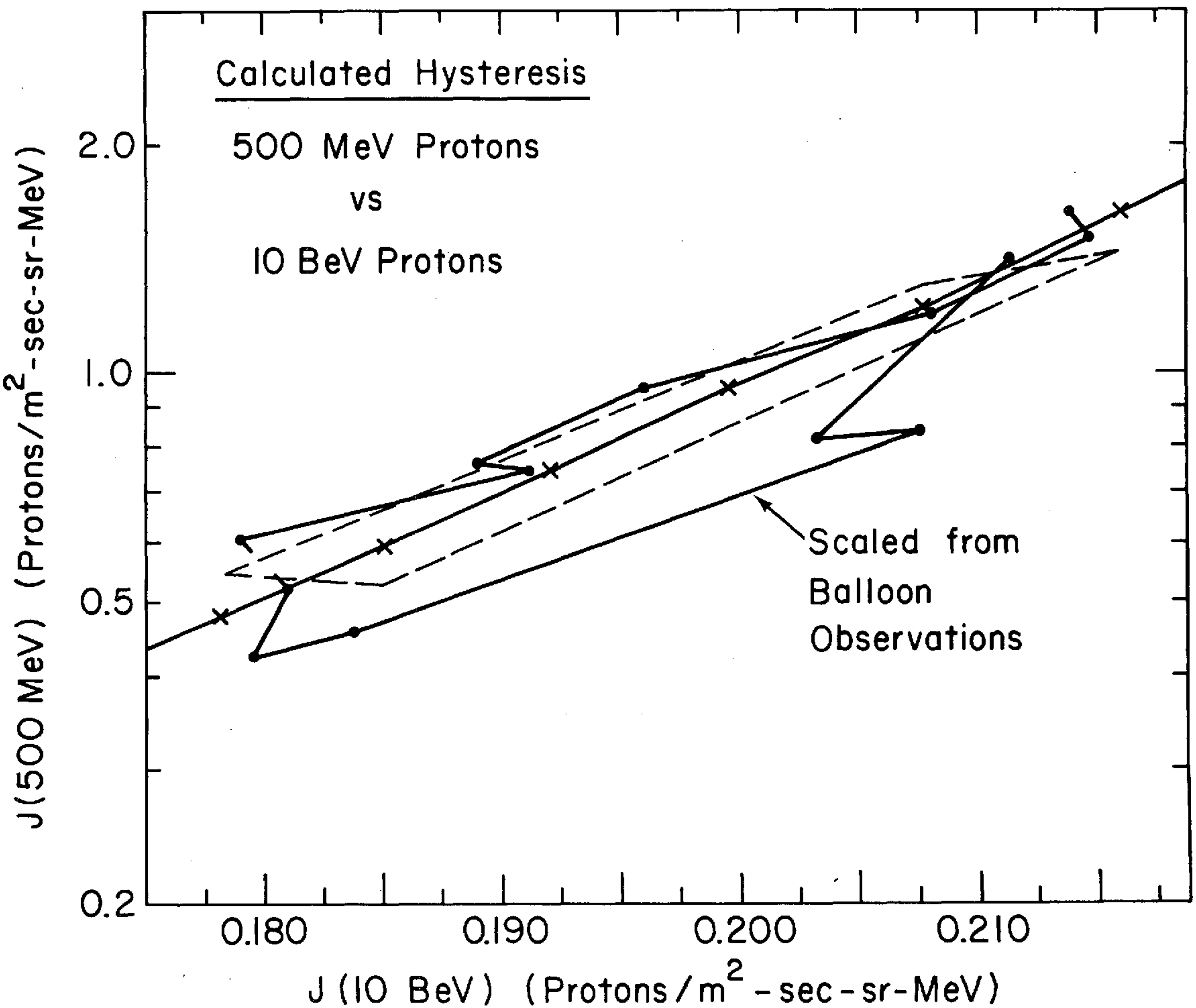
Calculated Hysteresis
500 MeV Protons
vs
10 BeV Protons
Scaled from
Balloon
Observations
2.0
1.0
0.5
0.2
J(500 MeV) (Protons/m2-sec-sr-MeV)
0.180
0.190
0.200
0.210
J (10 BeV) (Protons/m2-sec-sr-MeV)

FIGURE 8c